Austin Journal of Analytical & Pharmaceutical Chemistry

Open Access

Austin Publishing Group

Research Article

Synthesis of Zinc Oxide Nanoparticles (ZnO NPs) from Leaf Extract of *Carthamus oxycantha* and its In Vitro Biological Applications

Abdul Wahab[1]; Muhammad Waqas[1]; Sidra Urooj[2]; Hasnat Tariq[1]; Zeeshan Younas Abbasi[3]; Mohammad Ali[4]; Christophe Hano[5]; Bilal Haider Abbasi[1*]

[1]Department of Biotechnology, Quaid-i-Azam University, Pakistan

[2]Atta-U-Rehman School of Applied Biosciences (ASAB), National University of Science and Technology, Pakistan

[3]Department of Biological sciences, International Islamic University, Pakistan

[4]Centre for Biotechnology and Microbiology, University of Swat, Pakistan

[5]Institut de Chimie Organique et Analytique, Université d'Orléans, CNRS, France

***Corresponding author: Bilal Haider Abbasi**
Department of Biotechnology, Quaid-i-Azam University, Islamabad 45320, Pakistan.
Tel: +92-51-90644121
Email: bhabbasi@qau.edu.pk

Received: August 17, 2023
Accepted: October 02, 2023
Published: October 09, 2023

Abstract

Nanotechnology and nanosciences are emerging as new fast-growing fields due to their unique characteristics and phenomenal properties. In this study, we synthesized zinc oxide nanoparticles (ZnO NPs) by using leaf extract of Carthamus *oxycantha*. The morphological features of synthesized nanoparticles were evaluated by standard characterization techniques. The synthesized nanoparticles were irregular and hexagonal, and their average size was 11nm, as revealed by Scanning Electron Microscopy (SEM) and X-ray crystallography (XRD). Flavonoids and other phytochemicals were found to be capping metabolites for the nanoparticles. The synthesized nanoparticles showed significant inhibition of bacterial and fungal strains. The cytotoxicity assay showed 80% mortality of the marine larvae *Artemia salina* at a sample concentration of 40µg/ml. The crystallized ZnO NPs exhibited toxicity against MFC-7 breast cancer cells and displayed higher antioxidants profile i.e. free radical scavenging activity (76.824±1.22%), total reducing power (90.21±1.12µgAAE/mg), total antioxidant potential (72.936±0.93 µgAAE/mg). Quantity of 80 µg/ml of ZnO NPs resulted in 11.69±0.41% hemolysis against human red blood cells. Due to their potent biological activities, ZnO NPs synthesized from the leaf extract of *Carthamus oxycantha* could be used efficiently in transdisciplinary research in the future.

Keywords: *Carthamus oxycantha*; Zinc oxide nanoparticles; Green synthesis; Biological applications; Antioxidant activity; Anticancer activity

Introduction

Nanoscience and nanotechnology are rising as new emerging and fast-growing fields of science with diverse areas of applications in the manufacturing of various materials at the nanoscale [1]. Because of their phenomenal properties and unique characteristics, NPs have gained importance in various fields of sciences recently in a couple of year's i.e., energy sectors, health care fields, agriculture, environmental sciences, etc [2]. The green synthesis of NPs using bacteria [3], fungi [4], or other diverse varieties of plant [5-7] in recent years have emerged as a feasible and alternative methodology to more expensive and intricate procedures of chemical synthesis. Presently, metal nanoparticle synthesis has become the major site of attention in the research area of nanotechnology, and its combination with biological sciences provides new opportunities for the researchers to utilize it because of its remarkable applications in the areas of medicine, biomedical research, pharmaceuticals, drug delivery tools, and photocatalytic activities [8,9].

ZnO NPs acquire unique properties and astounding applications as compared to other metal NPs, such as in the field of medicine to manufacture sunscreen lotions (UV filters), anti-inflammatory, utilized for the detection of biomolecules [9], diagnosis [10], inhibition of microbial growth [11], catalytic activity [12] and carrier of antibiotics [12], healing of wounds, drug delivery techniques, transparent electronics, UV light emitters, piezoelectric devices and chemical sensors [13-17]. Therefore, regarding the background information of nanoparticles, a green synthesis approach is employed for the formation of ZnO NPs by using an aqueous extract of the *Carthamus oxycantha* plant due to its cost effectiveness, environmental friendliness and biocompatibility.

Plants are considered a key source for the synthesis of stable nanoparticles on a large scale. [18]. Phytochemicals present in different parts of the diverse plants' flora, i.e. roots, stems, and

Citation: Wahab A, Waqas M, Urooj S, Tariq H, Abbasi ZY, et al. Synthesis of Zinc Oxide Nanoparticles (ZnO NPs) from Leaf Extract of *Carthamus oxycantha* and its In Vitro Biological Applications. Austin J Anal Pharm Chem. 2023; 10(2): 1159.

leaves, help in the biosynthesis of NPs by acting as stabilizing and reducing agents; which gives a unique surface property to the NPs with a specific structure to enhance their practical applications [18,19]. Aqueous extract of plants contains natural biodegradable materials, which are eco-friendly and help in the development of non-toxic and cost-effective drugs at the nanoscale level [20].

Carthamus oxycantha (wild safflower, pohli) belongs to one of the largest flowering plant families "*Asteraceae*" which has1000 genera and about 10,000 species, spread over different areas in the world [21]. *C. oxycantha* is a bushy and annually grown medium-sized weed which has traditionally been used for medicinal purposes against a variety of diseases i.e. cough, typhoid, disorders related to the throat and heart, menstrual disorders, swelling, inflammation, anticoagulant, and cancer [22,23].

This study was aimed to design a plant-mediated eco-friendly and simple synthetic method for ZnO NPs by utilizing leaf extract of *Carthamus oxycantha* and to evaluate biological activities of the synthesized nanoparticles. To the best of our knowledge, this is the first study to synthesize ZnO NPs using the aqueous extract of *Carthamus oxycantha* leaves and their potent biological activities.

Materials and Methods

Collection of Plant

Fresh plants of *C. oxycantha* were collected from the south dessert area of Lakkimarwat, Khyber Pakhtunkhwa Province, Pakistan

Preparation of *Carthamus oxycantha* Leaves Extract

Leaves of *Carthamus oxycantha* were washed properly using distilled water, dried under shade and chopped up to a fine powder. Quantity of 10g of *Carthamus oxycantha* leaf powder was mixed with 60ml of distilled water. The mixture was retained in the water bath at 80˚C for 30 minutes. The mixture was kept on a magnetic stirrer after boiling for 30 minutes. The extract obtained was then filtered through Whatman No.1 filter paper.

Formation of Biosynthesized ZnO NPs

A solution of 2 mM zinc acetate was mixed with plant extract with a 4:1 ratio by following Thema et al. with slight modification [24]. The solution mixture was kept on a magnetic stirrer for 6 hours at 70˚C. The solution turned dark brown when the reaction was completed. The reaction mixture was centrifuged at 10,000 rpm for 15 minutes after 6hours of stirring to collect the precipitate/pellet. The resulting pellet was washed 3-4 times to remove the impurities. Later the pellet was dried out by pouring it on the Petri plate and incubated in a dry oven for 24 hours at 37˚C. When the ZnO NPs were finally made, they were ground up into a fine powder and stored for further analysis and characterization.

Characterization of Biosynthesized ZnO NPs

The optical properties of biosynthesized ZnO NPs were determined using a Perkin-Elmer lambda spectrophotometer. Reflectance spectra of prepared samples were obtained at room temperature at a range of wavelength 360-380nm. The crystalline structure of ZnO NPs was confirmed through X-Ray Diffraction (XRD) analysis in the 2θ range of 10˚- 40˚. PAN analytical Emprean Diffractrometer using CuKα radiation (λ=1.5406Å) and Bragg-Brentano θ-θ configuration. Morphology and elemental composition of biosynthesized ZnO NPs were determined by using a scanning electron microscope (SEM, NovaSEM450 operated at 20Kv) with Energy Dispersive X-ray (EDX) spectroscopy (IT100LA). Different chemical bonds present in biosynthesized ZnO NPs were identified by Fourier-Transform Infra-Red (FTIR) analysis within the 4000-515cm^{-1} range.

Biological Activities

Antioxidant Assay

DPPH Free Radical Scavenging Activity (FRSA)

DPPH free-radical scavenging activity was done as reported by [20]. Firstly, 3.2mg of 2,2-Diphenyl-1-Picryl Hydrazyl (DPPH) reagent was mixed with 100 mL of methanol. Sample concentrations of 20µg/ml, 40µg/ml, 60µg/ml, and 80µg/ml were mixed in 180µl of DPPH reagent solution. The mixture was thoroughly mixed before being incubated in the dark for an hour. Ascorbic acid served as a positive standard. Later, the absorbance of activity was taken using a spectrophotometer in a range of 514 nm.

The sample activity was analyzed by the following percentage formula,

Free Radical scavenging activity (%) = $[(A_c - A_s)/A_c] \times 100$

Where A_c is the absorbance of control and A_s is the absorbance of sample.

Total Reduction Potential (TRP)

The reducing power of ZnO NPs was investigated as previously mentioned in the literature [25]. 100µl of the sample was mixed with dH_2O to prepare a stock solution. Four different concentrations (20µg/ml, 40µg/ml, 60µg/ml, and 80µg/ml) were mixed in 200µl of Phosphate buffer (0.2M, pH=6.6) respectively and later 250µl of 1% potassium ferric cyanide was added. After proper mixing, the mixture was incubated in the water bath for 20 minutes at 50˚C. 200µl of 10% Trichloro-Acetic acid (TCA) was added to acidify the mixture. Later, centrifugation was done to separate the supernatant. 150µl of supernatant from the sample was mixed with 50µl of ferric chloride. Ascorbic acid was used as a positive control. The absorbance peak for the sample activity was analyzed by a microplate reader at 680nm.

Total Antioxidant Capacity Assay (TAC)

The total antioxidant activity (TAC) of ZnO NPs was analyzed by the following method [26]. Four different concentrations (20µg/ml, 40µg/ml, 60µg/ml, and 80µg/ml) of NP samples were prepared from the stock solution. 100µl of the sample was collected from the stock solution of each and mixed with 900µl of reagent TCA, which consists of 0.6M of sulfuric acid, 4mM ammonium molybdate, and 28mM sodium phosphate. After proper mixing of the solution, incubation was done at 95˚C for 90 minutes in the water bath. Later, the sample was cooled down at room temperature. The activity analysis was done at 695nm using a microplate reader. DMSO was taken as a negative and ascorbic acid was used as a positive control for curve calibration.

Total Flavonoid Content (TFC) Determination

For the determination of the TFC of ZnO NPs, the aluminum calorimetric method was followed according to [27] with a few

modifications. The stock solution was made by mixing 10% aluminum chloride and 1M potassium acetate in distilled water. Four different concentrations (20µg/ml, 40µg/ml, 60µg/ml, and 80µg/ml) of the NP sample were prepared. After that, 20µl of samples from respective concentrations were poured into a 96 well plate, to which 10µl of aluminum chloride, 10µl of potassium acetate, and 160µl of distilled water were added. The samples were then incubated for 30minutes at room temperature. Positive control was employed by taking 20µl of quercetin as a standard and 20µl of methanol as a negative control. The absorbance analysis of activity was measured by a microplate reader at 415nm.

Total Phenolic Content (TPC) Determination

For the determination of TPC of biosynthesized ZnO NPs, the procedure of [27] with slight changes was followed. The stock solution was made by mixing 4mg of ZnO NPs in 1ml of DMSO. 20µl of the sample was taken from stock and poured into a 96-well plate. Later, 90µl of Folin-Ciocalteu reagent and 90µl of sodium carbonate were added to respective wells containing test samples. The microplate was then incubated for 1 hr at room temperature and a reading was taken at 630nm using microplate reader. 20µl of Gallic acid, 90µl Fc reagent, 90 µl $NaCO_3$ as positive, and 20µl of DMSO as the negative standard were used.

Antibacterial Activity

The antibacterial activity of biosynthesized ZnO NPs was tested against four strains of bacteria by the disc diffusion method [28]. Two strains of gram-positive bacteria (*Klebsiella pneumonia* and *Staphylococcus aureus*) and two gram-negative bacterial strains (*Escherichia coli* and *Pseudomonas aeruginosa*) were studied. In this method, 4mg/ml of ZnO NPs were prepared in 1 ml of DMSO. After that, a sterile paper disk was soaked with a solution and was placed on the surface of agar plates on which pathogenic bacteria were inoculated. The plates were then incubated for 24hrs at 37°C. The diameters of the inhibition zones around the disks were measured as antibacterial activity. Positive and negative controls, Cefixime, and DMSO were used.

Antifungal Activity

Antifungal activity was tested against two fungal strains, including *Candida albicans* and *Aspergillus niger*, using the well diffusion technique following the protocol of [29]. The concentration of 4mg/ml of ZnO NPs sample wasutilized. Spores of fungal strains (0.1ml of each) were spread on a Sabouraud agar medium. Thereafter, 100µl of NP sample was transferred to a well plate. The plates were subsequently incubated at 37°C for 24hours and 32°C for 3 days. Biosynthesized ZnONPs samples were evaluated for their antifungal activity by measuring the zones of inhibition. Nilstat and DMSO were used as a positive and negative control, respectively.

Biocompatibility

The hemolytic activity assay RBCs-NPs interaction was conducted to evaluate the toxic nature of biosynthesized ZnO NPs using freshly obtained human blood. Approximately 1cc of blood was collected from volunteers (students) who had no other health issues. To prevent coagulation, blood was collected in an EDTA tube [30]. Blood was centrifuged at 14000rpm for 5 minutes to obtain fresh RBCs and separate plasma. RBCs were obtained in a pellet after 2-3 times centrifugation. Later, 9.8ml PBS (phosphate buffer saline) was added to 200µl of freshly obtained pellet erythrocytes. The solution in PBS was then thoroughly mixed by shaking it. NPs samples of four different concentrations (20µg/ml, 40µg/ml, 60µg/ml, and 80µg/ml, respectively) were added to suspended erythrocytes in a 1.5ml eppendorf tube. Then the mixture was incubated at 35˚C for 1hr. Then, afterward, the centrifugation of incubated sample was carried out at 10,000 rpm for 10 minutes. The supernatant was obtained, of which 100µl of it was poured into a 96-well plate. The absorbance of the obtained supernatant was measured at 541nm using a spectrophotometer. Triton X-10 was used as a standard positive control and DMSO as a negative control. The percentage hemolytic activity of RBCs is determined by the following formula,

$$\%\ Hemolysis\ =\ \frac{\{(sample\ abs\ -\ neg.\ control\ abs)\quad \times 100}{Positive\ control\ abs\ -\ negative\ control\ abs)\}}$$

Anticancer Activity

The anticancer activity of biosynthesized ZnO nanoparticles was tested against the breast cancer cell line MCF-7. The evaluation of cytotoxicity was done by MTT assay.

MTT Assay

Double serial dilutions of sample nanoparticles were made up to the 9th column of 96 well plates. The 10th column had cells+DMSO. The 11th column contained only cells, while DMSO was added to the 12th column. After incubation of cells with nanoparticles, 100µl of MTT dye was added to each well and incubated for 4hrs at 37\°C with 5% CO_2. Viable cells reduced the MTT dye to form crystals. After the incubation time, the media was removed carefully from each well without damaging the crystals. 100µl of DMSO was added to each well to solubilize the crystals. Then, the plate was placed in an incubator for 15 minutes at 37°C. Plates were read at 520nm using a plate reader. The percentage of cell viability was calculated by using the following formula:

$$\%\ Cell\ Viability\ =\ \frac{absorbance\ of\ sample\ -\ mean\ absorbance_{-ve\ control}}{Mean\ absorbance_{+ve\ control}}$$

The Evaluation of ZnO Nanoparticles Activity Against Dengue Virus on Vero Cells Cell Line

Vero cell line (CCL-81, ATCC) was used in this study. Vero cells are anchorage-dependent (adherent) and susceptible to a wide range of viral infections. Vero cell line is a proven model for Dengue virus experimentation [31]. The effect of biosynthesized ZnO nanoparticles on dengue virus is being explored in this study.

Co-Exposure Treatment

The co-treatment assay was performed to evaluate the function of nanoparticles in inhibiting viral binding. Vero cells were grown in a 96-well microliter plate with a flat bottom at 5000 cells/well. After the formation of a monolayer, the media was removed from all wells and 100µl of 100 TCID 50/ml viral suspension and different concentrations of nanoparticles (500ug, 250ug, 125ug, and 62.5ug) were added simultaneously to the cells in triplicate and incubated for 1h at 37°C. The virus and cell controls were also included in this assay. After incubation of 1h, the solution was discarded from the cells carefully. Then, the cells were washed three times with PBS. In each well, fresh complete medium was added. The plate was incubated for another 48hrs at 37°C with 5% CO_2.

Post-Exposure Treatment

In each well, 5000 cells were inoculated and allowed to grow until a monolayer was obtained. A flat-bottom 96-well plate

was used for this purpose. The confluent monolayer of Vero cells was incubated with 100µl of 100 TCID50/mL dengue virus (serotype 2) suspensions for 1 hour at 37°C in a CO_2 incubator with 5% humidity. Then, the virus inoculum was removed from the wells and the cells were washed three times with PBS to remove unattached viruses. Different concentrations of ZnO nanoparticles suspended in a growth medium were then added in triplicate to the wells and the plate was further incubated for 48hrs at 37°C with 5% CO_2. The virus control (virus + DMEM + cells) and the cell control (uninfected cells in DMEM) were also included in this experiment. In both co-exposure and post-exposure treatments, the morphology of cells was observed after 48hrs for each concentration of nanoparticles and compared to the level of efficacy of both treatments.

Brine Shrimp Lethality Assay

To test the mortality of ZnO nanoparticles, a 96-well microplate was used to perform the brine shrimp lethality assay. To hatch, the eggs of the test organism, *Artemia salina,* were incubated at 30–32°C for 24–48h in simulated seawater (38g/l supplemented with 6mg/l dried yeast), which was pre-saturated with oxygen. For this purpose, a specially designed tank with two compartments with a porous wall in between was used. In the bigger compartment, eggs were placed and covered with aluminum foil, and the smaller one was kept under constant illumination with the help of a lamp (the hatched nauplii (shrimp larvae) moved photo tropically to the other side through the pores). The Pasteur pipette was then used to harvest the nauplii and transferred to a small beaker (50ml) separately. From the beaker, the shrimp larvae (10 in number) were transferred to the 96 well microplates containing the samples in serial dilutions, and the volume was made up with seawater in such a way that the DMSO concentration remained less than 1%. The sample of ZnO NPs was tested at a concentration of 40µg/ml. The solutions of doxorubicin (4mg/ml DMSO) and DMSO served as positive and negative controls, respectively. After a period of 24hrs, the degree of lethality induced by each extract was quantified by taking into account the number of surviving larvae. The median Lethal Concentration (LC50) of the test samples with ≥50% mortality was calculated using graph pad prism software.

Results and Discussion

UV-Vis Spectrophotometer Analysis

The reduction of zinc by leaf extract of the *Carthamus oxycantha* to form ZnO NPs was confirmed through spectroscopy. Electrons in the conduction bands oscillated due to the effect of Surface Plasmon Resonance. A SPR peak was obtained in a range between 360nm - 380nm and showed confirmation of ZnO NPs formation after 24hrs of incubation (Figure 2) [18]. The bioactive compounds contained an extract of the *Carthamus oxycantha* plant, which reduced the Zn^{+2} to a zinc zero-valent Zn atom initially. The zero-valent Zn atom initiates the reduction of the remaining Zn^{+2} into ZnO and, finally, a cluster structure is obtained. ZnO NPs formation occurred by the reduction of zinc ions by the phytochemicals present in *Carthamus oxycantha* extract. These phytochemicals act as capping and stabilizing agents for stable ZnO NPs formation. The optical band-gap was calculated using Tauc`s equation

$$\alpha h\nu = k\,(h\nu - E_g)^n$$

where *k* is constt., hv is photon energy, E_g is energy gap, n=1/2 for allowed direct transition and n=2 is for indirect transition.

Analysis of X-ray Diffraction

The crystalline structure of biosynthesized ZnO nanoparticles was confirmed by X-ray diffraction. The crystal structure of nanoparticles is Wurtzite, in which the Oxygen (O) atoms are organized into a hexagonal close-packed type, with Zn atoms residing in half of the tetrahedral sites. Zinc (Zn) and Oxygen (O) atoms are in tetrahedral coordination with each other [25]. The hexagonal wurtzite structure of ZnO NPs was confirmed through the peaks at 2θ values of 32.9˚, 34.99˚, and 58.65˚ which corresponds to the crystalline planes of (100), (101), and (110) shown in (Figure 3) [32-34]. The average size was calculated at 11 nm using the Scherrer Debye equation [35].

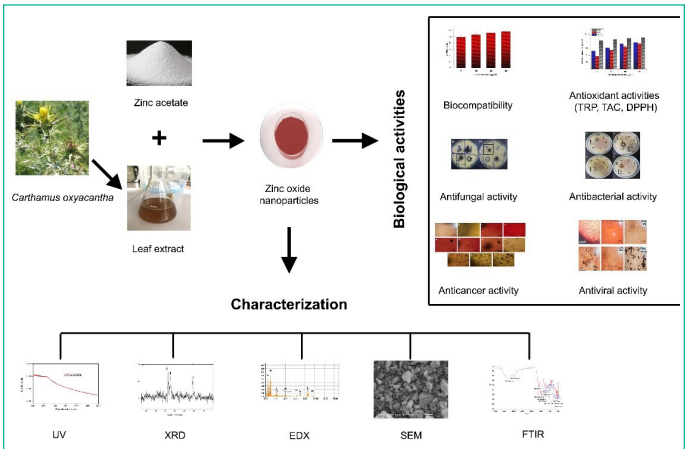

Figure 1: Graphical Abstract of Study.

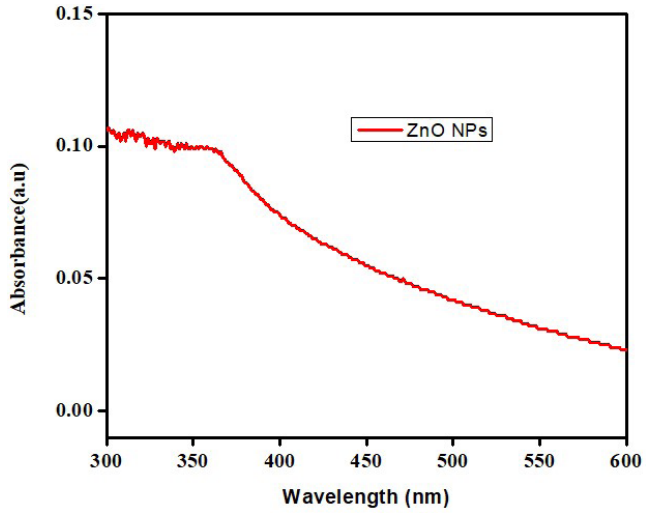

Figure 2: UV reflectance of biosynthesized ZnO NPs.

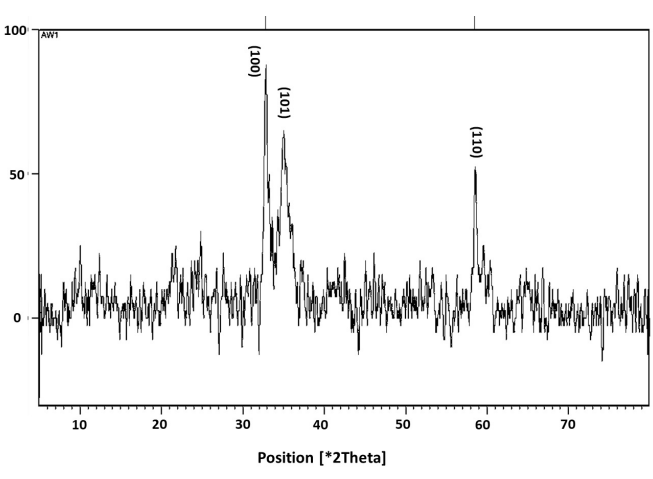

Figure 3: X-Ray Diffaractogram (XRD) of ZnO NPs.

FTIR Analysis

The presence of various organic compounds was confirmed by Fourier Transform Infra-red (FTIR) analysis as shown in (Figure 4). Absorption band peaks observed at 3394 cm^{-1} corresponded to alcohols, peaks at 1627 cm^{-1} corresponded to aldehydes; amines absorbed peaks at 3394.14; symmetric and asymmetric carboxylates were identified at peaks in the range of 1576-120 cm^{-1}. The absorption peaks observed at wave length numbers in the range of 400-600 cm^{-1} showed confirmation of ZnO NPs [18]. The peaks for (C=O) were observed at 1620 cm^{-1}, 574 cm^{-1} (O-H) bending, and in the range between 3400-3450 cm^{-1} (O-H) stretching. Absorption peaks observed in the range between 1543-1655 cm^{-1} showed the presence of (N-H) bonding of proteins or enzymes contained in the extract of *C. oxycantha* plant, Absorption peaks at 2850-2930 cm^{-1} corresponded to (C-H) stretching and 1116 cm^{-1} (C-H) plane bending. (C-O) bonding absorption peaks were observed at 1025 cm^{-1} and tetrahedral Zn coordination was observed at 857 cm^{-1}. The absorption peaks observed in the range of 1238-1080 cm^{-1} showed the presence of aliphatic and aromatic amines (C-N) bonds stretching. The presence of (N-H) and (O-H) bonding in the extract of the *C. oxycantha* plant revealed that phenolic compounds and proteins bio reduced Zn^{+2} into ZnO NPs.

SEM and EDX

Scanning Electron Microscopy (SEM) was used to identify the surface morphology of ZnO NPs. SEM analysis revealed irregular surface structures (rectangle, radial hexagonal, and spherical) of ZnO NPs (Figure 5A, 5B) as reported in the literature [36].

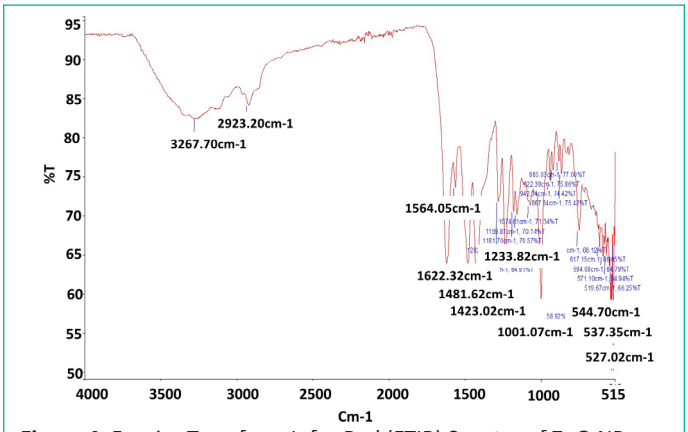

Figure 4: Fourier Transform Infra-Red (FTIR) Spectra of ZnO NPs.

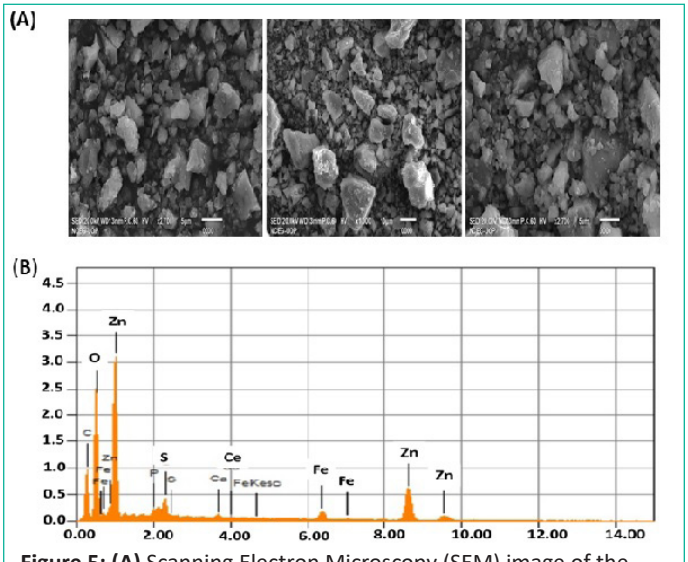

Figure 5: (A) Scanning Electron Microscopy (SEM) image of the biosynthesized ZnO NPs **(B)** Energy Dispersive X-ray (EDX) spectra of ZnO NPs.

Energy Dispersive X-ray (EDX) spectra were used to evaluate the surface chemical composition of biosynthesized ZnO NPs. Three clear signals for zinc (Zn) and one for each C, O, and P were observed. Other peaks for elements such as Fe, Ca, and S were also observed. The signals of extra peaks in the EDX spectrum for C, P, S, Ca, and Fe show the presence of phytochemicals on the surface of ZnO NPs synthesized from the leaf extract of *C. oxycantha.*

Biological Activities

Antioxidant Potential (DPPH, TRP, TAC)

A DPPH reagent was used to determine the percent free Radical Scavenging Activity (RSA) of the nanoparticles and plant extracts. The method is based on the DPPH (purple in color) being reduced to a stable diphenyl by accepting hydrogen from an antioxidant donor, and the picrylhydrazine molecule (yellow in color) is formed. Free radical antioxidant activity indicates the capacity of synthesized NPs to scavenge free radicals. Antioxidants are a prominent source to get rid of free radicals and protect from illness and other health issues caused by these reactive species [37]. To assess the Total Antioxidant Capacity (TAC), a phosphatemolybdenum-based approach was used, which depends on an antioxidant mediator converting Mo(VI) to Mo(V), resulting in the production of a phosphate-molybdate complex, which is identifiable by its green color and TRP based on transforming the Fe^{+3} to Fe^{+2} ion is produced by the tested sample if it possesses redox capacity [38].

In these assays, ZnO NPs samples were applied and analyzed with different concentrations (20µl/ml, 40µl/ml, 60µl/ml, and 80µl/ml) while ascorbic acid was taken as the positive standard represented in the (Figure 6). The antioxidant potential shown by all samples in the experiment is dose dependent, highest activity at 80 µg/ml are DPPH 76.824±1.22 FRSA%, TRP 90.21±1.12µg AAE/mg and TAC 72.936±0.93µg AAE/mg, respectively. The reason for the antioxidant activity of *C. oxycantha* leaf extract may be the presence of bioactive phytochemicals such as flavonoids, alkaloids, and phenolic compounds in it.

Total Flavonoid Content and Total Phenolic Content

TFC and TPC were determined using the aluminum calorimetric method as reported previously [39]. The phenolic and flavonoid contents of aqueous extract of *C. oxycantha* plant and biosynthesized ZnO NPs are presented in the Table 1.

Table 1: TFC and TPC of *Carthamus oxycantha* extract and biosynthesized ZnO NPs.

	Flavonoid contents (mg/l)	Phenolic contents (mg/l)
Extract	22.314±0.041	26.33±0.067
ZnO NPs	4.13±0.024	6.82±0.053

Table 2: Hemolytic activity of biosynthesized ZnO NPs treated Human RBCs.

Concentrations (µg/ml)	%Hemolysis
80	11.69±0.041
60	11.29±0.038
40	10.69±0.035
20	9.89±0.036

Data presented is ± SE of three measurements.

Table 3: Brine Shrimp Lethality Assay of Biosynthesized ZnO NPs.

Concentrations		%Mortality	
(µg/ml)	ZnO	Doxorubicin	DMSO
20	35±0.034	30±0.022	10±0.03
40	50±o.04	40±0.03	20±0.011
60	80±0.032	50±0.043	25±0.078

Note: DMSO = Negative Control; Doxorubicin = Positive Control;3 Data presented is **± SE** of three measurements

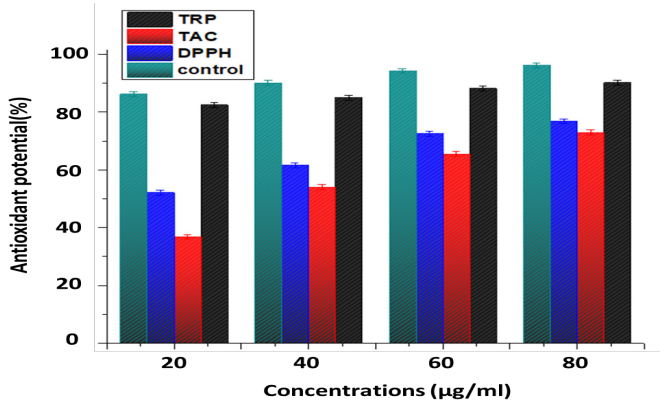

Figure 6: Antioxidant potential of biosynthesized ZnO NPs.

Antimicrobial Activity

The antibacterial and antifungal activities of biosynthesized ZnO NPs are presented in (Figure 7) and (Figure 8), respectively. The bactericidal effect of biosynthesized ZnO NPs was found to be higher against gram-positive strains as compared to gram-negative strains due to structural differences [40]. ZnO NPs revealed efficient zones of inhibition for *P.* aeruginosa (7mm), *E. coli* (10mm), *S. aureus* (7mm) and *K. pneumonia* (7mm). Similar results were previously reported in the literature with higher zone of inhibition against *E. coli* [41]. ZnO NPs also exhibited fungicidal effects against *C. albicans* and *A. niger* with zone of inhibition of 13.5mm and 15mm respectively.

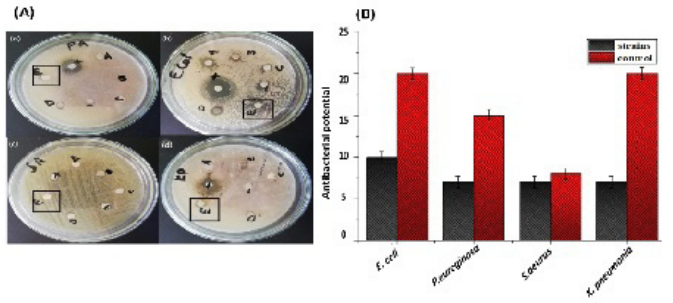

Figure 7: Antibacterial activity of biosynthesized ZnO NPs **(A)** activity shown on petri plates (Zno NPs in black) **(a)** *Pseudomonas aeurogonos* **(b)** *Eschercia coli* **(c)** *Staphylococcus aureus* **(d)** *Klebsbilla pneumonia* **(B)** graphical presentation of activity.

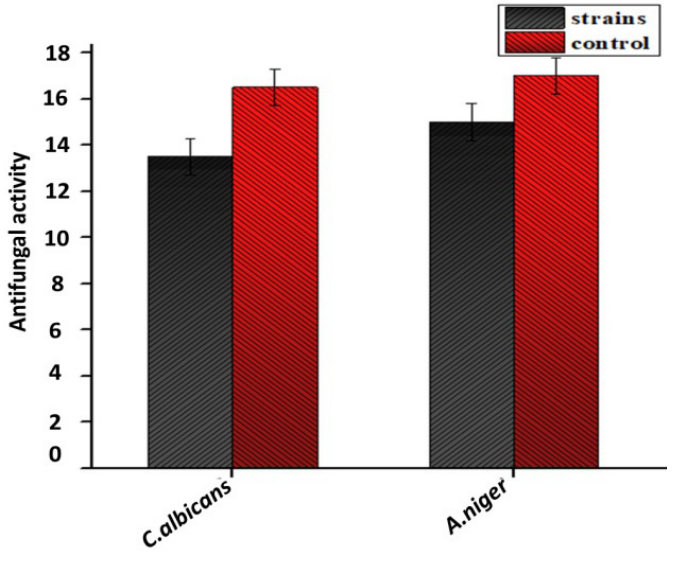

Figure 8: Antifungal activity of biosynthesized ZnO NPs (*Aspergilus niger, Candida albicans*).

Biocompatibility

The biocompatibility assay showed that the synthesized ZnONPs were non-toxic to normal human cells. The hemolytic activity of NPs was determined and compared to the finding values according to the standard of "American Society for Testing and Materials Designation". Based on these standards, any type of NPs or other material having ≥5% hemolysis is considered hemolytic, others having 2-5% are mild hemolytic, while having ≤2% is considered safe and non-hemolytic [43]. The hemolysis activity of NPs was measured upon the rupturing of RBCs and release of hemoglobin to the medium when treated with different concentrations of ZnO NPs (80µg/ml, 60µg/ml, 40µg/ml, and 20µg/mg). In comparison to previous studies, the current study revealed that ZnO NPs are hemolytic [44].

Anticancer Activity

The cytotoxicity of biosynthesized ZnO NPs against the MCF-7 breast cancer cell line was tested *in vitro*, as shown in (Figure 9). The results showed that the cytotoxic activity against cancer cells increased with increasing ZnO NP concentration. The findings were compared to previous reports [45]. It was discovered that as the concentration of ZnO NPs increased, more ZnO NPs accumulated in cancer cells, causing cell death. The specific target mechanism and action of nanoparticles make them highly desirous for use in cancer therapy. Zinc plays a crucial role in cell cycle regulation, DNA replication, DNA repair, and apoptosis. It is evident that changes in zinc concentration in cancer cells may have deleterious effects. Disequilibrium in protein functions and oxidative stress [46] are key factors mediated by Zn and involved in cancer cell death. Apart from the Enhanced Permeability and Retention (EPR) effect, electrostatic interactions are also responsible for the target-specific killing of cancer cells [47].

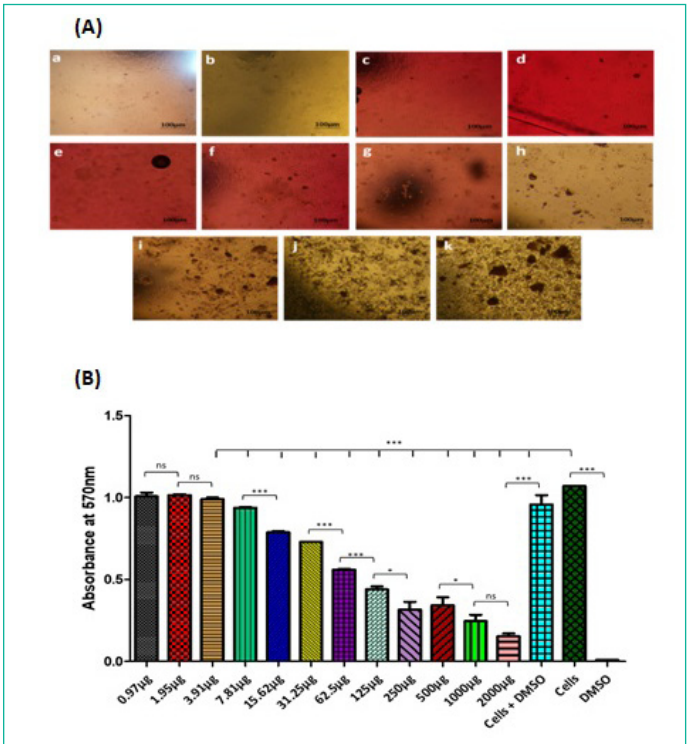

Figure 9: Anticancer activity of biosynthesized ZnO nanoparticles against MCF-7 breast cancer cell line **(A)** Pictorial presentation of ZnO NPs cytotoxicity against MCF-7 breast cancer cells (**a**)0.97 µg (**b**)1.95 µg (**c**)3.91 µg (**d**) 7.81 µg (**e**) 15.62 µg (**f**) 31.25 µg (**g**) 62.5 µg (**h**) 125 µg (**i**) 250 µg (**j**) 500 µg (**k**) 1000 µg **(B)** Graphical presentations of viability of MCF-7 breast cancer cells against different concentrations of biosynthesized ZnO NPs employed.

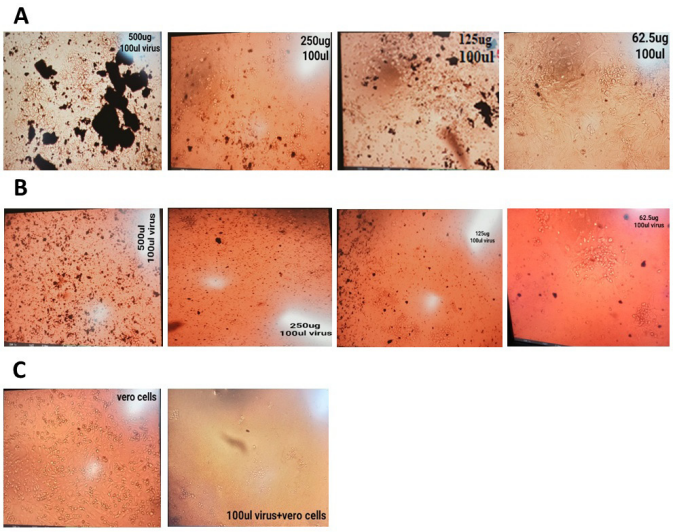

Figure 10: Antiviral activity of biosynthesized ZnO nanoparticles against dengue virus on Vero cells. **(A)** Post-exposure treatment **(B)** Co-exposure treatment **(C)** Virus and cells control.

Antiviral Activity

This research has been conducted to examine the ability of ZnO NPs (11nm) to inhibit the dengue virus. Vero cells were used for *in vitro* dengue virus propagation. Nanoparticles exert their striking antiviral effects when added after viral infection of the cells. A significant decrease in viral titer had been examined after nanoparticle exposure. Most favorable results have been shown in (Figure 10) through post-exposure treatment [48] and a concentration of 62.5 µg is more effective in providing striking effects against virus and more number of viable cells [49]. Existing knowledge on nanoparticle interaction with viruses suggests that nanoparticles bind to DENV and could inhibit its binding by preventing receptor-epitope covalent interactions [50].

Brine Shrimp Lethality Assay

The solubility of ZnO NPs in seawater and its toxicity towards *Artemia salina* larvae is employed to elaborate its chemical and toxicological impact on marine microorganisms. The mortality of biosynthesized ZnO NPs is mentioned in table 3. The lethality concentrations of ZnO NPs used were 20 µg/ml, 60 µg/ml, and 80 µg/ml. The lethality was directly proportional to the sample concentration. The lowest lethality was observed at a concentration of 20 µg/ml which was 35%. The results demonstrated that lethality is concentration-dependent and that biosynthesized ZnO NPs are highly cytotoxic to brine shrimp [51].

Conclusion

In the current study, ZnO nanoparticles were successfully biosynthesized from *Carthamus oxycantha* leaf extract. The green synthesis methodology for ZnO nanoparticles was described as reproducible, reusable, environmentally friendly, and non-toxic. According to the findings of this study, the green synthesis of nanoparticles can be safe, simple, cost-effective, and environmentally friendly. The use of biological materials as precursors for the biosynthesis of nanoparticles has received increased attention in the field of nanotechnology and has had a significant impact on nano-science advancements. ZnO nanoparticles produced biologically have a wide range of biological applications, including antifungal, antiviral, antibacterial, and anticancer activity. Biosynthesized ZnO nanoparticles have a significant antioxidant capacity and efficient brine shrimp lethality activity, as determined *in vitro*. Biosynthesized ZnO nanoparticles also demonstrated strong hemolytic activity against human red blood cells. On the basis of these applications and biological activities, biosynthesized NPs may be used in the future for a wide range of medical care and treatments.

Author Statements

Author Contributions

BHA and AW contributed to the main idea, conceptualization and performing the research work. MW contributed in the data collection and analysis. MW and HT have contribution in formatting the manuscript draft and creating figures and tables. SU performed formal analysis, ZYA and CH help in manuscript proofreading. All authors have read and agreed to the published version of the manuscript.

Funding

This research received no external funding.

Acknowledgments: We are grateful to Department of biotechnology, Quaid I Azam University Islamabad, Pakistan for providing research facilities.

Conflicts of Interest

The authors declare no conflict of interest.

References

1. Albrecht MA, Evans CW, Raston CLJGc. Green chemistry and the health implications of nanoparticles. 2006; 8: 417-32.
2. Martínez G, Merinero M, Pérez-Aranda M, Pérez-Soriano EM, Ortiz T, Begines B, et al. Environmental impact of nanoparticles' application as an emerging technology: a review. Materials (Basel). 2020; 14: 166.
3. Joerger R, Klaus T, Granqvist CGJAM. Biologically produced silver–carbon composite materials for optically functional thin-film coatings. Adv Mater. 2000; 12: 407-9.
4. Shankar SS, Ahmad A, Sastry MJBp. Geranium leaf assisted biosynthesis of silver nanoparticles. Biotechnol Prog. 2003; 19: 1627-31.
5. Shankar SS, Ahmad A, Pasricha R, Sastry M. Bioreduction of chloroaurate ions by geranium leaves and its endophytic fungus yields gold nanoparticles of different shapes. J Mater Chem. 2003; 13: 1822-6.
6. Chandran SP, et al. Synthesis of gold nanotriangles and silver nanoparticles using Aloe vera plant extract. 2006; 22: 577-83.
7. Gardea-Torresdey JL, Parsons JG, Gomez E, Peralta-Videa J, Troiani HE, et al. Formation and growth of Au nanoparticles inside live alfalfa plants. 2002; 2: 397-401.
8. Basnet P, Inakhunbi Chanu T, Samanta D, Chatterjee S. A review on bio-synthesized zinc oxide nanoparticles using plant extracts as reductants and stabilizing agents. J Photochem Photobiol B. 2018; 183: 201-21.
9. Sharmila G, Sakthi Pradeep R, Sandiya K, Santhiya S, Muthukumaran C, Jeyanthi J, et al. Biogenic synthesis of CuO nanoparticles using Bauhinia tomentosa leaves extract: characterization and its antibacterial application. Journal of Molecular Structure. 2018; 1165: 288-92.
10. Munje RD, Muthukumar S, Prasad S. Lancet-free and label-free diagnostics of glucose in sweat using zinc oxide based flexible bioelectronics. Sensors and Actuators B: Chemical. 2017; 238: 482-90.

11. Azizi S, Mohamad R, Bahadoran A, Bayat S, Rahim RA, Ariff A, et al. Effect of annealing temperature on antimicrobial and structural properties of bio-synthesized zinc oxide nanoparticles using flower extract of Anchusa italica. J Photochem Photobiol B. 2016; 161: 441-9.

12. Soto-Vázquez L, Cotto M, Morant C, Duconge J, Márquez F. Facile synthesis of ZnO nanoparticles and its photocatalytic activity in the degradation of 2-phenylbenzimidazole-5-sulfonic acid. Journal of Photochemistry and Photobiology A: Chemistry. 2017; 332: 331-6.

13. Stan M, Popa A, Toloman D, Dehelean A, Lung I, Katona G. Enhanced photocatalytic degradation properties of zinc oxide nanoparticles synthesized by using plant extracts. Materials Science in Semiconductor Processing. 2015; 39: 23-9.

14. Sravanan R, Devaraj M, Qin J, Naushad M, Gracia F, et al. Mechanothermal synthesis of Ag/TiO2 for photocatalytic methyl orange degradation and hydrogen production. 2018; 120: 339-47.

15. Wang ZL. Zinc oxide nanostructures: growth, properties and applications. J Phys.: Condens Matter. 2004; 16: R829-58.

16. Wahab R, Mishra A, Yun SI, Kim YS, Shin HS. Antibacterial activity of ZnO nanoparticles prepared via non-hydrolytic solution route. Appl Microbiol Biotechnol. 2010; 87: 1917-25.

17. Akhtar MS, Ramzan A, Ali A, Ahmad M. Effect of Amla fruit (Emblica officinalis Gaertn.) on blood glucose and lipid profile of normal subjects and type 2 diabetic patients. Int J Food Sci Nutr. 2011; 62: 609-16.

18. Sharmila G, Farzana Fathima M, Haries S, Geetha S, Manoj Kumar N, Muthukumaran C. Green synthesis, characterization and antibacterial efficacy of palladium nanoparticles synthesized using Filicium decipiens leaf extract. Journal of Molecular Structure. 2017; 1138: 35-40.

19. Bharathi D, Vasantharaj S, Bhuvaneshwari VJMRE. Green synthesis of silver nanoparticles using Cordia dichotoma fruit extract and its enhanced antibacterial, anti-biofilm and photo catalytic activity. Mater Res Express. 2018; 5: 055404.

20. Velsankar K, Aswin Kumar RM, Preethi R, Muthulakshmi V, Sudhahar S. Green synthesis of CuO nanoparticles via Allium sativum extract and its characterizations on antimicrobial, antioxidant, antilarvicidal activities. Journal of Environmental Chemical Engineering. 2020; 8: 104123.

21. Ahmad R, Jilani G, Arshad M, Zahir ZA, Khalid A. Bio-conversion of organic wastes for their recycling in agriculture: an overview of perspectives and prospects. Ann Microbiol. 2007; 57: 471-9.

22. Majumder P, Mazumder S, Chakraborty M, Chowdhury SG, Karmakar S, Haldar PK. Preclinical evaluation of Kali Haldi (Curcuma caesia): a promising herb to treat type-2 diabetes. Orient Pharm Exp Med. 2017; 17: 161-9.

23. Tariq SL, Ali HM, Akram MA, Janjua MM, Ahmadlouydarab M. Nanoparticles enhanced phase change materials (NePCMs)-A recent review. Applied Thermal Engineering. 2020; 176: 115305.

24. Thema FT, Manikandan E, Dhlamini MS, Maaza M. Green synthesis of ZnO nanoparticles via Agathosma betulina natural extract. Materials Letters. 2015; 161: 124-7.

25. Javed M, Ahmad I, Usmani N, Ahmad M. Studies on biomarkers of oxidative stress and associated genotoxicity and histopathology in Channa punctatus from heavy metal polluted canal. Chemosphere. 2016; 151: 210-9.

26. Haq IU, Chaudhry WN, Akhtar MN, Andleeb S, Qadri I. Bacteriophages and their implications on future biotechnology: a review. Virol J. 2012; 9: 9.

27. Jafri SAA, et al. Evaluation of some essential traditional medicinal plants for their potential free scavenging and antioxidant properties. 2023; 35: 102562.

28. Shah M, Nawaz S, Jan H, Uddin N, Ali A, Anjum S, et al. Synthesis of bio-mediated silver nanoparticles from Silybum marianum and their biological and clinical activities. Mater Sci Eng C Mater Biol Appl. 2020; 112: 110889.

29. Ahmad K, Khalil AT, Somayya R. Antifungal, phytotoxic and hemagglutination activity of methanolic extracts of Ocimum basilicum. J Tradit Chin Med. 2016; 36: 794-8.

30. Khalil AT, Ovais M, Ullah I, Ali M, Shinwari ZK, Khamlich S, et al. Sageretia thea (Osbeck.) mediated synthesis of zinc oxide nanoparticles and its biological applications. Nanomedicine (Lond). 2017; 12: 1767-89.

31. Medina F, et al. Dengue virus: isolation, propagation, quantification, and storage. 2012; 27: 15D.

32. Rajabi HR, Naghiha R, Kheirizadeh M, Sadatfaraji H, Mirzaei A, Alvand ZM. Microwave assisted extraction as an efficient approach for biosynthesis of zinc oxide nanoparticles: synthesis, characterization, and biological properties. Mater Sci Eng C Mater Biol Appl. 2017; 78: 1109-18.

33. Thakuria H, Borah BM, Das G. Macroporous metal oxides as an efficient heterogeneous catalyst for various organic transformations—a comparative study. 2007; 274: 1-10.

34. Vanathi P, Rajiv P, Narendhran S, Rajeshwari S, Rahman PKSM, Venckatesh R. Biosynthesis and characterization of phyto mediated zinc oxide nanoparticles: a green chemistry approach. Materials Letters. 2014; 134: 13-5.

35. Borchert H, Shevchenko EV, Robert A, Mekis I, Kornowski A, Grübel G, et al. Determination of nanocrystal sizes: a comparison of TEM, SAXS, and XRD studies of highly monodisperse CoPt3 particles. Langmuir. 2005; 21: 1931-6.

36. Umar H, Kavaz D, Rizaner NJIjon. Biosynthesis of zinc oxide nanoparticles using Albizia lebbeck stem bark, and evaluation of its antimicrobial, antioxidant, and cytotoxic activities on human breast cancer cell lines. Int J Nanomedicine. 2019; 14: 87-100.

37. Jegadeesan GB, Srimathi K, Santosh Srinivas N, Manishkanna S, Vignesh D. Green synthesis of iron oxide nanoparticles using Terminalia bellirica and Moringa oleifera fruit and leaf extracts: antioxidant, antibacterial and thermoacoustic properties. Biocatalysis and Agricultural Biotechnology. 2019; 21: 101354.

38. Prieto MA, Curran TP, Gowen A, Vázquez JA. An efficient methodology for quantification of synergy and antagonism in single electron transfer antioxidant assays. Food Research International. 2015; 67: 284-98.

39. Jafri SAA, Khalid ZM, Khan MZ, Jogezai N. Evaluation of phytochemical and antioxidant potential of various extracts from traditionally used medicinal plants of Pakistan. Open Chemistry. 2022; 20: 1337-56.

40. Emami-Karvani Z, PJAJMR. Chehrazi, antibacterial activity of ZnO nanoparticle on gram-positive and gram-negative bacteria. 2011; 5: 1368-73.

41. Rajabi M, Mousa SAJB. The role of angiogenesis in cancer treatment. Biomedicines. 2017; 5: 34.

42. Sharmila G, Bhat FA, Arunkumar R, Elumalai P, Raja Singh P, Senthilkumar K, et al. Chemopreventive effect of quercetin, a natural dietary flavonoid on prostate cancer in in vivo model. Clin Nutr. 2014; 33: 718-26.

43. Aula S, Lakkireddy S, Swamy AVN, Kapley A, Jamil K, et al. Biological interactions in vitro of zinc oxide nanoparticles of different characteristics. 2014; 1: 035041.

44. Ali T, Tripathi P, Azam A, Raza W, Ahmed AS, et al. Photocatalytic performance of Fe-doped TiO2 nanoparticles under visible-light irradiation. 2017; 4: 015022.

45. Alishah H, Pourseyedi S, Ebrahimipour SY, Mahani SE, Rafiei N. Green synthesis of starch-mediated CuO nanoparticles: preparation, characterization, antimicrobial activities and in vitro MTT assay against MCF-7 cell line. Rend Fis Acc Lincei. 2017; 28: 65-71.

46. Bisht G, Rayamajhi SJN. ZnO nanoparticles: a promising anticancer agent. Nanobiomedicine (Rij). 2016; 3: 3-9.

47. Khaleghi S, Khayatzadeh J, Neamati AJMT. Biosynthesis of zinc oxide nanoparticles using Origanum majorana L. leaf extract, its antioxidant and cytotoxic activities. Materials Technology. 2022; 37: 2522-31.

48. Kelley WJ, Zemans RL, DRJERJ. Goldstein, cellular senescence: friend or foe to respiratory viral infections?. 2020; 56.

49. Kinney RM, Huang CY, Rose BC, Kroeker AD, Dreher TW, Iversen PL, et al. Inhibition of dengue virus serotypes 1 to 4 in vero cell cultures with morpholino oligomers. J Virol. 2005; 79: 5116-28.

50. Wade D, Diaw PA, Daneau G, Camara M, Dieye TN, Mboup S, et al. CD4 T-cell enumeration in a field setting: evaluation of Cy-Flow counter using the CD4 easy count kit-dry and Pima CD4 systems. PLoS One. 2013; 8: e75484.

51. Supraja N, Prasad TNVKV, Gandhi AD, Anbumani D, Kavitha P, Babujanarthanam R. Synthesis, characterization and evaluation of antimicrobial efficacy and brine shrimp lethality assay of Alstonia scholaris stem bark extract mediated ZnONPs. Biochem Biophys Rep. 2018; 14: 69-77.